# Ultra low-cycle fatigue modeling of welded joints under multi-axial strain conditions for better seismic design

**Dr. Gary S. Prinz**
Steel Structures Laboratory (ICOM), École Polytechnique Fédérale de Lausanne

**Prof. Dr. Alain Nussbaumer**
Steel Structures Laboratory (ICOM), École Polytechnique Fédérale de Lausanne

## 1. Introduction

When ductile steel systems fail during earthquakes, they tend to fail near connection regions and often under ultra low-cycle fatigue (ULCF) conditions. To determine connection fatigue capacities for design, static-cyclic laboratory tests on connection assemblies or components are often used; however, the complicated multi-axial stress states that exist under real earthquake loading are rarely applied during such tests. With maximum distortion strain energy theory suggesting that multi-axial strain states may reduce the effective yield of materials, there exists the possibility for increased connection fatigue damage under multi-axial strain conditions.

This paper presents an example method for investigating welded T-joint connection capacities under multi-axial loads, considering low-cycle fatigue fracture initiation as the primary limit state. Welded T-joint connections can be found in many structures, including seismic resitant steel frames and steel liquid storage tanks, and therefor results presented herein are applicable to many situations. The paper begins by discussing modeling techniques and model validation methods based on previous experimental testing. The discussion describes a preliminary control model representing a steel liquid storage tank connection. Then, several test models designed to determine the effects of multi-axial loads are presented, along with key results.

## 2. Modeling Methods

Boundary conditions and loading for the T-joint models in this study are based on the experimental setup and welded liquid-storage tank connection geometry described in (Cortes, 2011), creating a control model whereby analytical methods can be validated with experimental result. The control model connection has an applied tensile stress perpendicular to the weld direction (hereafter referred to as a perpendicular-tensile stress, $\sigma_{11}$) equal to 50% of yield ($50\%\sigma_y$), along with repeatedly applied bending stress cycles simulating an uplifting tank base during an earthquake. The complete dimensions for the control model plates are 300x160x6mm. While in reality, tank connections are subjected to both parallel-tensile and perpendicular-compressive stresses at

the connections, only perpendicular tensile stresses were included in the experimental test setup.

Boundary constraints and applied stresses simulated the supporting structure and hydraulic actuators used in the experiment. All model constraints are shown in Figure 1. ABAQUS was used for the analysis (HKS, 2006).

Solid elements and a refined mesh modeled the steel plates and fillet welds (see Figure 2). Eight node solid elements with reduced integration (C3D8R in ABAQUS) were used in the entire model. For increased strain accuracy near the welded connection, element sizes were decreased providing several elements through the T-joint thickness. S355 material properties were assigned to the plates and fillet welds. Large displacement effects were accounted for using the nonlinear geometry option in ABAQUS.

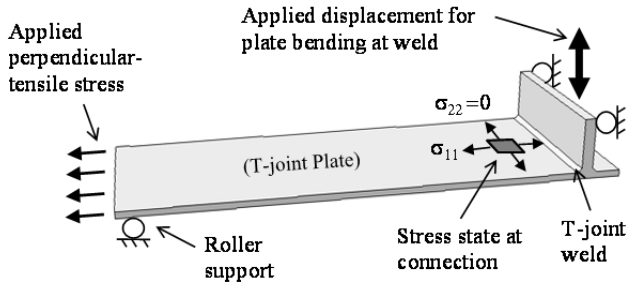


Figure 1: T-joint model constraints

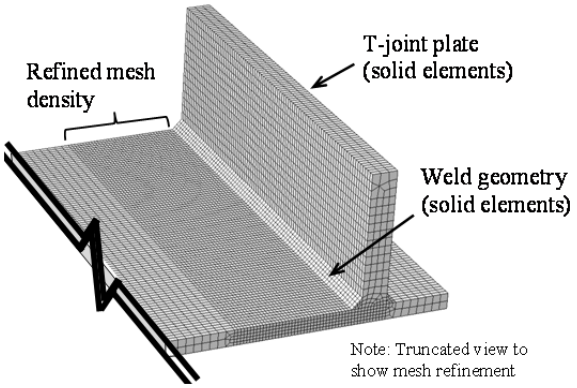


Figure 2: Element type and mesh refinement

## 3. Fatigue Damage Model

A low-cycle fatigue failure index based on a stress modified critical strain (SMCS) criterion is used to estimate the connection rotation capacity in each model. The failure index is computed as the accumulated equivalent plastic strain, $\bar{\varepsilon}_P$, divided by a critical plastic strain, $\varepsilon_{p,critical}$. This critical plastic strain was theoretically derived by Hancock and Mackenzie (Hancock, 1976) as:

$$\varepsilon_{\mathrm{p,critical}} = \alpha \ \exp\left(-\frac{3\sigma_m}{2\sigma_e}\right) \qquad (1)$$

where $\sigma_m$ is the hydrostatic stress, $\sigma_e$ is the von Mises stress, and $\alpha$ is a material toughness index. Fracture initiation is indicated when the failure index ($\bar{\varepsilon}_P / \varepsilon_{p,critical}$) exceeds 1.0. Several researchers have used this criterion to investigate ductile fracture (Kanvinde, 2006; Shih-Ho Chao, 2006; Prinz, 2010), and it is used in this study since the T-joints are expected to undergo ultra low-cycle fatigue (failure after only a few loading cycles).

To calibrate $\alpha$ in Equation 1, four CNT specimens of S355 steel were fabricated from the control experiment specimen and tested to failure in tension according to ASTM Standard *E8* (ASTM, 2002). The resulting $\alpha$ value was 2.84 and is used for all analyses in this study. See (Myers, 2010) for the detailed $\alpha$ calibration procedure and (Prinz, 2010) for the determination of the $\alpha$ parameter used in this study.

## 4. Test Models and Analysis Matrix

In addition to the control model, 23 models were analyzed considering T-joint connections under multi-axial loading. The same modeling techniques and plate geometry were used for the test models as described for the control model, but additional compressive stresses acting parallel with the weld (hereafter referred to as parallel-compressive stresses, $\sigma_{22}$) were added to the plate edges. Along with the constant perpendicular and parallel planar stresses, the 23 test models were loaded by applying repeated bending cycles at three levels of plate rotation (0.3, 0.4, and 0.5rad). Table 1 shows the analysis matrix along with the performance parameter used to investigate multi-axial loading effects (the number of cycles required to reach a failure index of 1.0,hereafter referred to as $N_{f1}$). Results from the multi-axial models are discussed later in the Results section.

| Model | Perpendicular Weld Stress, $\sigma_{11}$ [$\%\sigma_y$] | Parallel Weld Stress, $\sigma_{22}$ [$\%\sigma_y$] | $N_{f1}$[a] | | |
|---|---|---|---|---|---|
| | | | $\theta_{max}$[b]=0.3 [rad] | $\theta_{max}$=0.4 [rad] | $\theta_{max}$=0.5 [rad] |
| C0 | 50 | 0 | 3.9[c] | 2.6 | 1.8 |
| C1 | 50 | 10 | 3.8 | 2.6 | 1.7 |
| C2 | 50 | 15 | 3.6 | 2.6 | 1.7 |
| C3 | 50 | 20 | 3.6 | 2.6 | 1.7 |
| D0 | 10 | 0 | 30.9 | 12.8 | 8.8 |
| D1 | 10 | 5 | 19.0 | 11.8 | 8.0 |
| D1 | 10 | 10 | 17.0 | 10.8 | 7.7 |
| D2 | 10 | 15 | 15.9 | 9.9 | 6.9 |

[a] Number of cycles to reach failure index of 1
[b] Applied peak rotation
[c] Control Model

Table 1: Analysis matrix and performance parameter (Nf1)

## 5. Results

### 5.1. Modeling Validation from Control Experiment

Comparison between the control model and experiment focused on localized low-cycle fatigue near the connection region. Fatigue analysis of the control model closely matched experimental data and observation. Figure 3 shows the failure index plot of the

control model, along with the observed experiment failure. In Figure 3, predicted ($N_{f1}$) and actual failure occurred on the same rotation half-cycle (near 3-1/2 cycles at 0.3rad for both the experiment and control model).

## 5.2. Fatigue-Life Capacity Curves

For connection design purposes it is useful to relate connection rotation and $N_{f1}$. Figure 4 shows the resulting fatigue-life capacity curves for each applied stress state, plotted in log-log scale assuming a Cofin-Manson power law relationship. From Figure 4, the T-joint (tank connection) could be expected to achieve near 7 cycles at 0.5 rad with 10%$\sigma_y$ perpendicular-tensile stress and 20%$\sigma_y$ parallel-compressive stress applied to the base-plate.

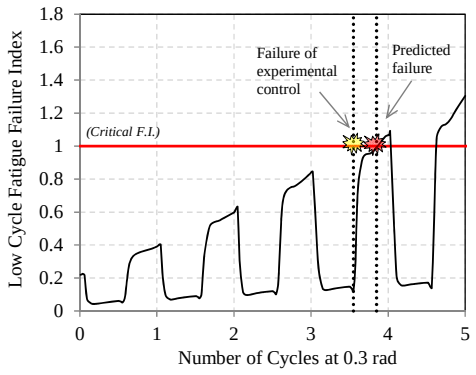


Figure 3: Failure index for control model compared with experimental failure

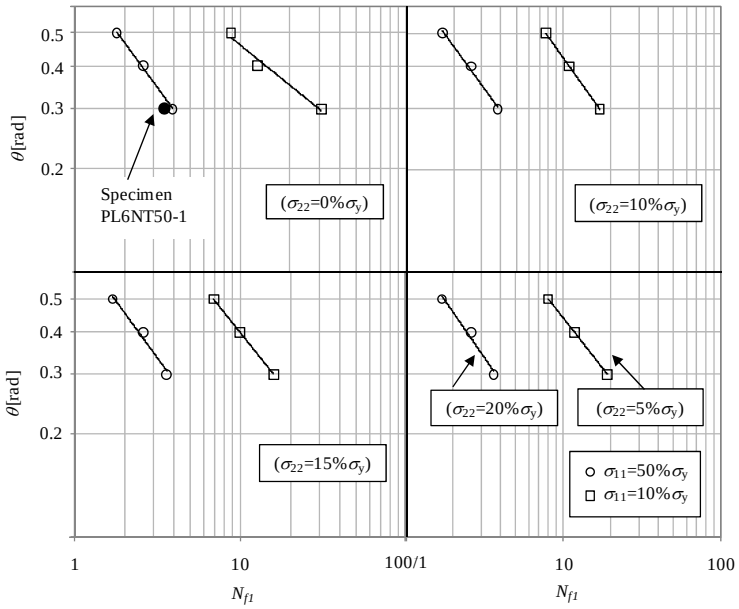


Figure 4: Fatigue-life curves for different stress states (amounts of perpendicular-tensile and parallel-compressive stress)

## 5.3. Effect of Perendicular-Tensile and Parallel-Compressive stresses on Plastic Strain Accumulation

Combined perpendicular-tensile and parallel-compressive stresses decrease connection rotation capacity by increasing plastic strain accumulations in the plate next to the weld. Figure 5 shows the accumulated equivalent plastic strain in the T-joint plate under various amounts of perpendicular-tension and parallel-compression. As expected, plastic strain increased with increases in parallel compressive stress; however, for models having lower perpendicular-tensile stress (10%$\sigma_y$), the increase in plastic strain due to parallel-compressive stress was higher (between 13% and 38% higher on average depending on the peak rotation 0.5rad or 0.3rad) (see Figure 3). Model D1 having a peak rotation of 0.3rad

had a 41% increase in plastic strain with 10% increase in parallel-compressive stress. This is directly related with the reduction in fatigue capacity reported in Table 1, which is not surprising given the heavy influence of plastic strain on the low-cycle fatigue failure index.

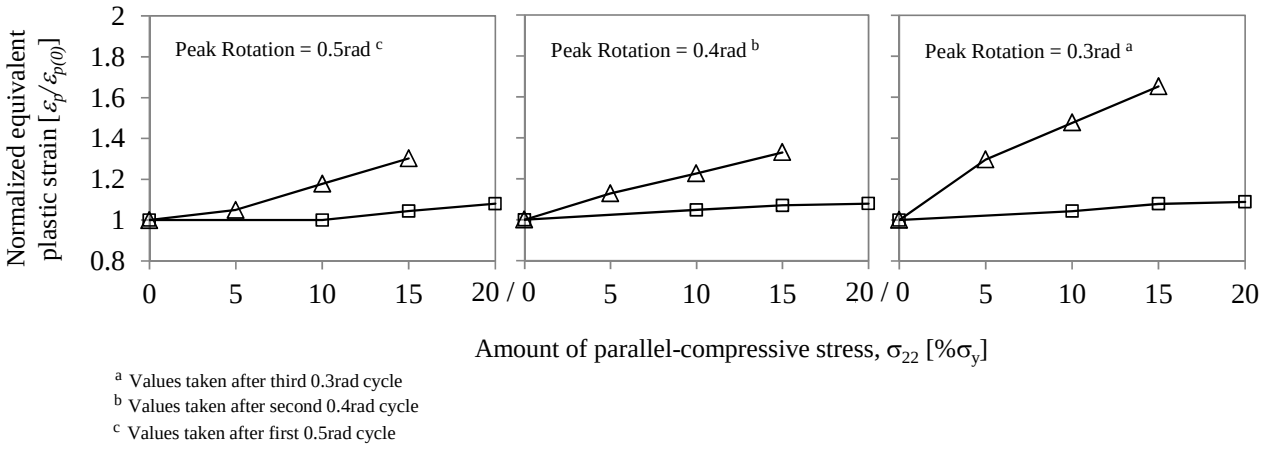


[a] Values taken after third 0.3rad cycle
[b] Values taken after second 0.4rad cycle
[c] Values taken after first 0.5rad cycle

Figure 5: Normalized equivalent plastic strain versus amount of parallel-compressive stress, for peak rotations of 0.3, 0.4, and 0.5rad

## 6. Summary and Conclusion

In this study, methods for investigating the effects of multi-axial stresses on the low-cycle fatigue of welded T-joints (representing liquid storage tank connections) were presented. A finite element control model was first validated using experimental results and a low-cycle fatigue failure index. Then twenty-three additional connection models having 6mm plate thicknesses and varied multi-axial stress states were subjected to repeated rotations of 0.3, 0.4, and 0.5rad. The following conclusions are based results from the static cyclic analysis of the twenty-four welded connections:

1. The SMCS ductile fracture criterion is a reasonably good predictor of ULCF fracture in welded T-joints subjected to bending.
2. Plate parallel-compressive stresses ($\sigma_{22}$) have the greatest effect on plastic strains and connection ULCF ($N_{f1}$) when perpendicular-tensile stresses ($\sigma_{11}$) and connection rotations are low.
3. Smaller rotation cycles may contribute more to connection fatigue in tank connections, than previously reported in Cortes et al [15], due to increased plate yielding from moderate parallel-compressive and perpendicular-tensile stresses.
4. The fatigue-life curves presented in this study provide an estimation of connection capacity for 6mm thick welded T-joint connections under various multi-axial stress-states.

## 7. References


ASTM (2002). Standard test methods for tension testing of metallic materials. E8, . West Conshohicken, Pa.

Cortes, G., Nussbaumer, A., Berger, C., and Lattion, E. (2011). "Experimental determination of the rotational capacity of wall-to-base connections in storage tanks." *J. Constructional Steel Research,* **67**(2011): 1174-1184.

Hancock, J. W., and Mackenzie, A.C. (1976). "On the mechanics of ductile failure in high-strength steel subjected to mulit-axial stress-states." *J. Mech. Phys. Solids* **24**(3): 147-160.

HKS (2006). "ABAQUS Standard Users manual, Version 6.4." Hibbitt, Karlsson, and Sorensen, Inc.

Kanvinde, A. M., and Deierlein, G.G. (2006). "Void growth model and stress modified critical strain model to predict ductile fracture in structural steels." *J. Struct. Eng.* **132**(12): 1907-1918.

Myers, A. T., Kanvinde, A.M., and Deierlein, G.G. (2010). "Calibration of the SMCS criterion for ductile fracture in steels: specimen size dependence and parameter assessment." *J. Eng. Mech.* **136**(11): 1401-1410.

Prinz, G. S., and Nussbaumer, A. (2010). "Fatigue analysis of unanchored liquid storage-tank shell-to-base connections under multi-axial loading." *Eng. Structures*.

Prinz, G. S., and Richards, P.W. (2010). "Eccentrically braced frame links with reduced web sections." *J. Constructional Steel Research* **65**(2009): 1971-1978.

Shih-Ho Chao, K. K., and Sherif El-Tawil (2006). "Ductile web fracture initiation in steel shear links." *J. Struct. Eng.* **132**(8): 1192-1200.